Oxidation of Metals, Vol. 25, Nos. 5/6, 1986

The Healing Behavior of Protective Oxide Scales on Heat-Resistant Steels After Cracking Under Tensile Strain

M. Schütze*

Received July 26, 1985

The healing of cracks in protective oxide scales on four heat-resistant steels has been investigated at 800°C in constant-extension-rate tests, in metallographic and in SEM-examinations. The experimental results suggest the existence of a critical strain rate below which crack healing leads to an instant repair of the cracked scale thus preventing increased internal corrosion. The existence of this critical strain rate can be explained by model considerations, the results of which are in agreement with the results from the experiments. On the basis of scale cracking data from a previous paper and healing data in the present paper "scale cracking/healing maps" have been developed characterizing the protective capabilities of the oxide scales under tensile strain.

KEY WORDS: heat-resistant steels; oxide-scale crack healing; protective capabilities; constant-extension-rate tests.

INTRODUCTION

In a previous paper[1] the cracking behavior of the protective oxide scales on four heat-resistant steels and on Ni99.6 had been investigated in tensile tests at constant strain rates from 10^{-6} to 10^{-9} s^{-1} and at a temperature of 800°C. The results from these investigations showed that the strains to the beginning of scale cracking were comparatively low and did not exceed 0.5% unless lateral oxide growth effects reduced the tensile stresses in the scales. It was concluded from these results that under service conditions strains of the order of magnitude leading to scale cracking cannot be avoided in every case.

*Dechema-Institut, D-6000 Frankfurt/M.97, West Germany.

0030-770X/86/0600-0409$05.00/0

Table I. Chemical Composition of the Alloys Tested (wt.%)

	C	P	Si	Ti	Cr	Mn	Fe	Ni	Al	S	Cu	Ce
18Cr steel	0.066	0.018	1.48		18.19	0.50	r.		0.80	0.006		
18Cr-Ce steel	0.12	0.048	1.50		18.7	1.00	r.		1.14	0.012		0.12
24Cr steel	0.088	0.033	0.97		24.12	0.57	r.		1.41	0.003		
Alloy 800	0.070		0.37	0.44	20.99	0.99	r.	33.50	0.26	0.005	0.60	

Scale cracking, however, need not inevitably lead to an irreversible loss of the protective effect of oxide scales if crack-healing processes occur. In the case that a protective oxide scale grows via outward migration of metal cations a scale crack may be closed again by the formation of new oxide[2]. If the scale grows by inward diffusion of oxygen the protective effect may also be restored, but in this case the original scale-crack contours are preserved while an oxide wedge extends into the base metal at the cracked site.[2] Oxide wedges, however, might have a negative influence on the mechanical performance of the material and are thus undesired.

As already mentioned in Ref. 1, a most conservative assessment of the limits to the protective effect of scales under tensile stresses would not allow any scale cracking for the protective case. Since under service conditions, however, oxide-scale cracking cannot be excluded, the knowledge of the healing behavior of scale cracks becomes of great importance.

In the following the results from the investigations of the oxide scales on the heat-resistant steels in Ref. 1 shall be viewed under the aspect of scale crack healing. These steels were three ferritic alloys (18 Cr steel, 18 Cr-Ce steel, and 24 Cr steel) and the austenitic Alloy 800 (32 Ni20 Cr Steel). The composition of these steels is given in Table I. The scales on the ferritic steels consisted predominantly of alumina with additional partial layers of chromia and Cr-Mn-oxide (the sequence of the partial layers from the inside to the outside is alumina/chromia/Cr-Mn-oxide). On Alloy 800 the main layer was chromia with partial layers of silica (at the inside) and Cr-Mn-oxide (at the outside). Details can be taken from Ref. 1.

EXPERIMENTAL EVIDENCE OF SCALE CRACK HEALING

Direct evidence of healing processes after scale cracking under tensile deformation could be found in surface investigations as well as in investigations of metallographic sections. Examples of healed cracks as observed in

surface investigations are shown in Figs. 1 and 2. With decreasing strain rates it becomes more difficult to recognize healed cracks on the surfaces (compare Figs. 1 and 2). Figure 3 shows an example of healed cracks in a metallographic section. The characteristic contours of the cracks which do not penetrate the entire scale allow the assumption to be made that these cracks are in the state of healing. If these contours were the consequence of stable crack growth in the scale, extensive plastic deformation would have been necessary which can be excluded according to former observations.[1] Cracks and healed cracks could be found after certain strains on all materials investigated with the exception of the ferritic 18Cr-Ce steel. The latter always exhibited a smooth oxidized surface, although the results from the acoustic emission measurements had indicated scale cracking. It is assumed that crack healing occurs extremely rapid in this case.

Besides the optical evidence of healed scale cracks, results from investigations of internal oxidation as well as the nitriding of Al in ferritic steels and internal oxidation of Al preferentially along grain boundaries in Alloy 800 all suggest that healing processes occurred in the scales. This is shown

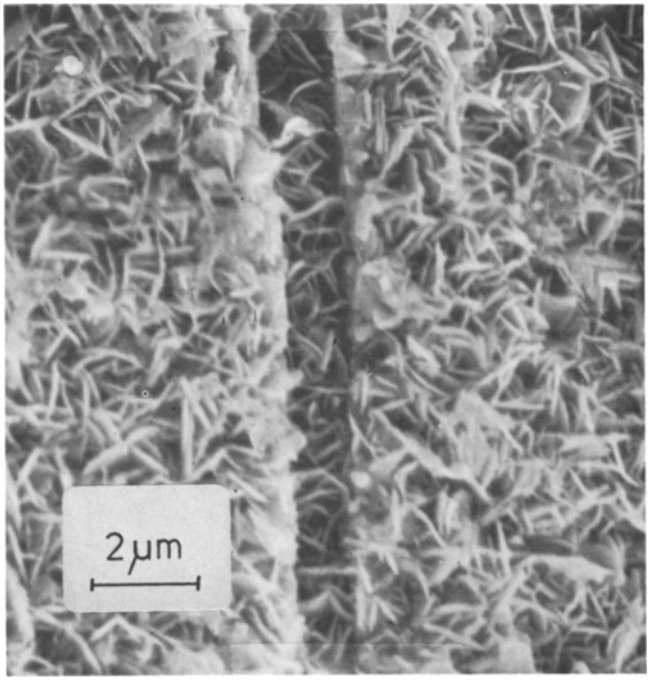

Fig. 1. SEM micrograph of a partially healed crack in the oxide scale of Alloy 800 after deformation at 800°C (strain rate $10^{-6}\,s^{-1}$).

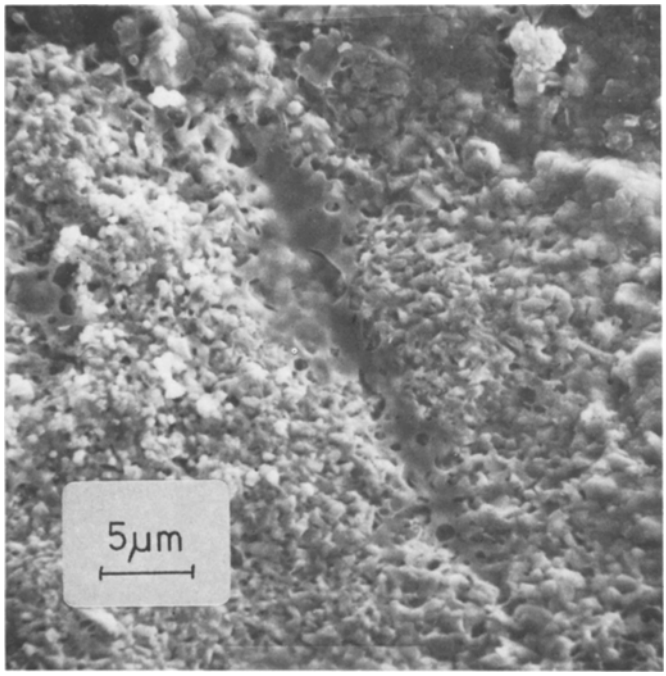

Fig. 2. SEM micrograph of a healed crack in the oxide scale of Alloy 800 after deformation at 800°C (strain rate $10^{-8}\,s^{-1}$).

in Fig. 4. There the course of internal corrosion as a function of time is shown for specimens deformed at a strain rate $\dot{\varepsilon}_0$ of $10^{-8}\,s^{-1}$ and for undeformed specimens of the 18 Cr steel, the 24 Cr steel and Alloy 800. Time t and strain at the beginning of scale cracking are indicated by the arrows. The 18 Cr steel shows a marked increase of internal corrosion in deformed specimens soon after the beginning of scale cracking, whereas, no severe increase is found for the 24 Cr steel and Alloy 800 at this strain rate, although scale cracking had occurred several times. For strain rates of 10^{-6} and $10^{-7}\,s^{-1}$ it had been observed that internal corrosion increases in deformed specimens of these three alloys soon after the beginning of scale cracking.[1] For the 18 Cr-Ce steel no internal corrosion had been found over the investigated strain-rate region. We may conclude from these facts that a critical strain rate seems to exist, below which increased internal corrosion is suppressed by rapid healing of oxide-scale cracks and above which the healing rates are too low compared to the deformation rates, so that increased internal corrosion cannot be prevented. The values of these critical strain rates should lie below $10^{-8}\,s^{-1}$ for the 18 Cr steel, between

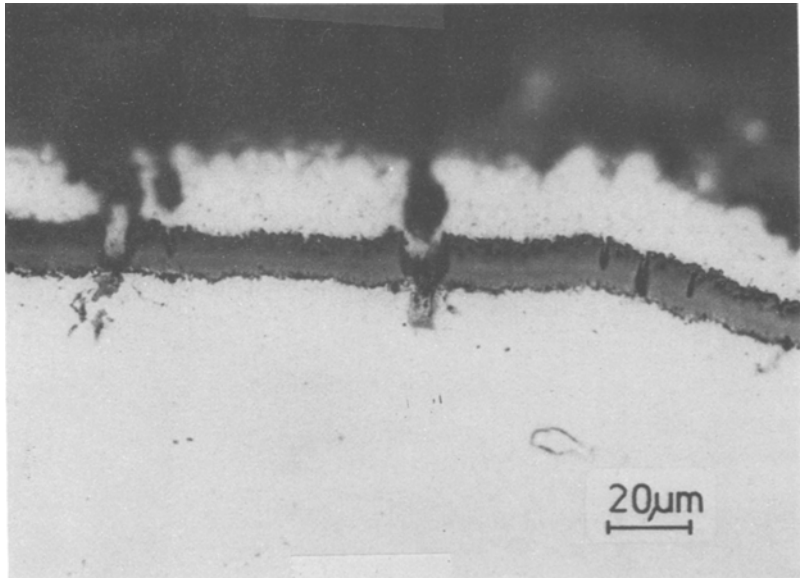

Fig. 3. Examples of partially healed cracks in the oxide scale on Alloy 800 (metallographic section).

10^{-7} and $10^{-8}\,s^{-1}$ for the 24 Cr steel and Alloy 800, and above $10^{-6}\,s^{-1}$ for the 18 Cr-Ce steel.

Critical strain rates for the increase of corrosion have been observed also in the literature. Creep-rupture tests at 650°C in water vapor showed for Incoloy 800 that corrosion was enhanced above a strain rate of about $3 \cdot 10^{-9}\,s^{-1}$.[3] A critical strain rate of about $10^{-6}\,s^{-1}$ had been found in creep tests with Fe-20Cr-12Ni and Fe-17Cr-6Ni at 900°C in air.[4] From creep-rupture tests in an oxidizing/carburizing atmosphere with Incoloy 800 and Incoloy 802 at 1000°C, it was estimated that the critical strain rate should lie below $10^{-8}\,s^{-1}$ in this case.[5]

MODEL-LIKE CONSIDERATIONS ON THE CRITICAL STRAIN RATE FOR CRACK HEALING

As already mentioned, closing up of a scale crack by healing will be possible if a scale grows predominantly by the outward diffusion of metal cations. In this case the oxide-growth rate, dx/dt, is dependent on the length of the diffusion paths, x, for the cations according to

$$dx/dt = k_p/x \qquad k_p = \text{parabolic rate constant of oxide growth} \qquad (1)$$

In a cracked scale oxide growth will occur not only on the outer oxide

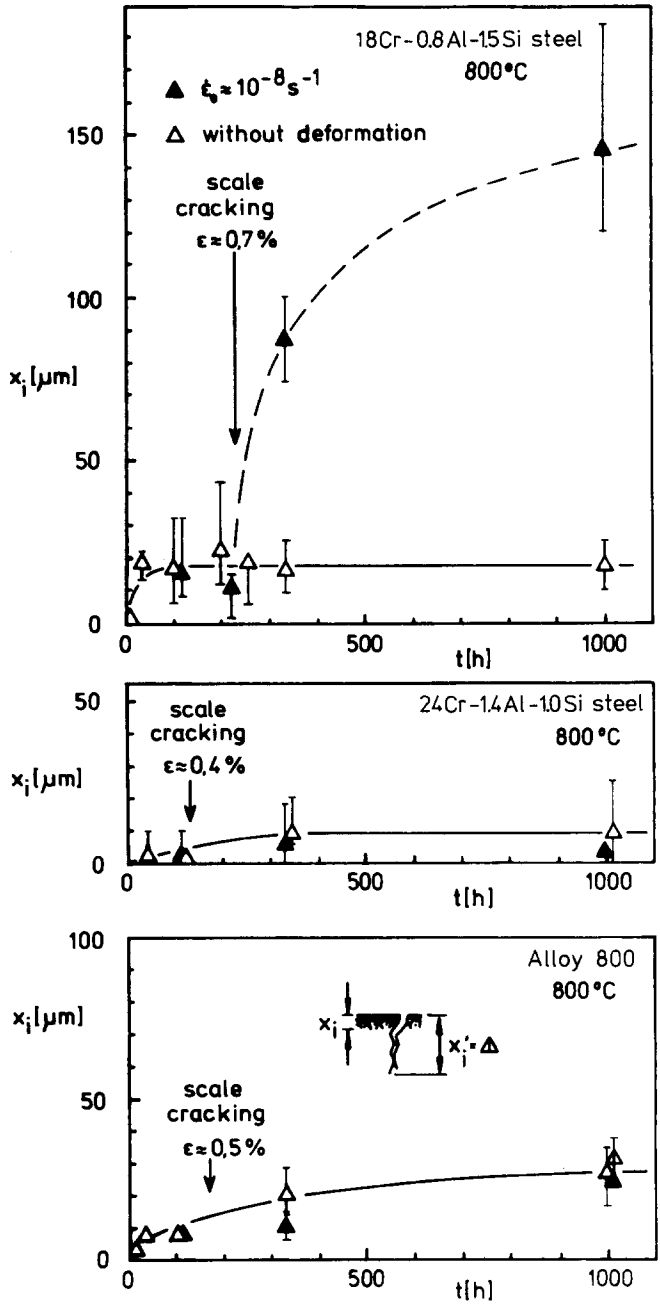

Fig. 4. Depth of internal corrosion as a function of time and strain/time values for the beginning of scale cracking (arrows) at a strain rate of $10^{-8}\,s^{-1}$.

surfaces but also at the scale-crack faces (in the lateral direction) and at the bottom of the crack on the metal surface. In Fig. 5 this situation is shown schematically. At the crack faces oxide growth is faster toward the oxide-metal interface than at the oxide-gas interfaces according to Eq. (1). The resulting course of the growth rate at the crack faces as a function of the distance from the metal (approx. x) is shown on the right side of Fig. 5. The scale-crack contours which develop by these oxide-growth processes are indicated schematically by the dashed lines.

Restoration of the protective effect by crack healing can be assessed by a comparison between the rate at which the crack faces are moved apart by substrate deformation and the growth rate at the crack faces which results in closure of the cracks in the tensile direction (in the following estimation oxide growth from the bottom of the scale crack is neglected). Oxide growth in the tensile direction occurs on the faces of n cracks in the gauge length, i.e., there are $2n$ crack faces contributing to an oxide "length increase" l_{ox} in the tensile direction:

$$dl_{0x}/dt = 2n \cdot k_p/x \tag{2}$$

The respective "healing rate" $\dot{\varepsilon}_H$ amounts to

$$\dot{\varepsilon}_H = dl_{0x}/l_0 dt = 2k_p/x \cdot l_R$$

l_0 = gauge length of the specimen before straining

l_R = distance between the oxide scale cracks ($l_R \approx l_0/n$) (3)

Now a critical value of the strain rate $\dot{\varepsilon}_0^H$ can be calculated at which the applied strain rate $\dot{\varepsilon}_0$ equals the healing rate $\dot{\varepsilon}_H$, i.e., at strain rates below this value instant crack healing should occur. In order to include the possible strain-rate dependence of l_R, Eq. (4) is used for the calculations:[1]

$$l_R \propto \dot{\varepsilon}_0^m \qquad m = 0 \cdots -0.5 \tag{4}$$

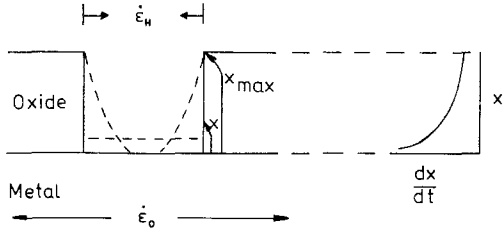

Fig. 5. Schematic illustration of the scale crack healing process.

The critical strain rate $\dot{\varepsilon}_0^H$ (i.e., the strain rate at which $\dot{\varepsilon}_0 = \dot{\varepsilon}_H$) results from the following calculations:

$$\dot{\varepsilon}_0^H = \dot{\varepsilon}_0 = \dot{\varepsilon}_H = 2k_p / l_R \cdot x \qquad (5)$$

If a value l_R^1 at a strain rate $\dot{\varepsilon}_0^1$ is known from measurements the other l_R-values can be calculated by:

$$l_R = l_R^1 (\dot{\varepsilon}_0 / \dot{\varepsilon}_0^1)^m \qquad (6)$$

Insertion of Eq. (6) into Eq. (5) yields:

$$\dot{\varepsilon}_0^H = (2k_p \cdot \dot{\varepsilon}_0^{1^m} / x \cdot l_R^1)^{1/(m+1)} \qquad (7)$$

This critical strain rate $\dot{\varepsilon}_0^H$ represents a minimum value below which instant formation of new oxide between the scale-crack faces with a thickness x should be guaranteed. Actually the critical strain rate below which the protective effect is maintained may be higher, because oxide growth also occurs from the bottom of the scale cracks which has been neglected in this estimation.

APPLICATION OF THE MODEL TO EXPERIMENTAL RESULTS

The values which are needed for the estimation of the critical strain rates, according to the calculations in the preceding section, can be taken out of Ref. 1. These values are listed in Table II for the 18 Cr steel, the 24 Cr steel, and Alloy 800. The investigations had, however, not provided the necessary values for the 18 Cr-Ce steel which is not included in the following considerations. The values of x in Table II represent the scale thickness after longer testing times when no further, strong increase in scale thickness occurs. It is assumed that these values are equal to the maximum lengths of the diffusion paths for the metal cations in the scales, if the scales are adherent. For the two ferritic steels which had shown oxide wrinkling, combined with local scale detachment, two different values of x are given

Table II. Values from Investigations[1] for the Calculation of $\dot{\varepsilon}_0^H$

	$k_p(m^2/s)$	$\dot{\varepsilon}_0^1(s^{-1})$	$l_R^1(\mu m)$	m	$x(\mu m)$
18 Cr steel	1×10^{-17}	10^{-6}	100	−0.27	(a) 5
					(b) 50
24 Cr steel	9×10^{-18}	10^{-6}	100	−0.27	(a) 2
					(b) 5
Alloy 800	2×10^{-17}	10^{-6}	50	−0.26	(a) 7

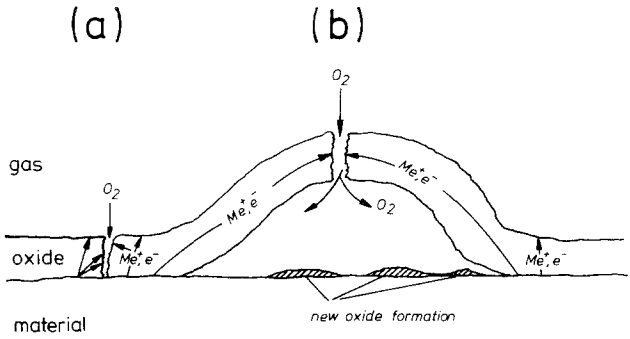

Fig. 6. Transport processes during the healing of cracks in scales.

in Table II. One stands for the adherent parts of the scale (a) (x = scale thickness) and the other for the detached top of the convolutions (b). The latter represents the length of the diffusion path from adherent parts of the scale to the top of the convolutions as measured in scales at $\dot{\varepsilon}_0 = 10^{-8}\,s^{-1}$. A schematic representation showing the diffusion paths in adherent parts of the scale (a) and in detached regions (b) is given in Fig. 6.

The results obtained by inserting the values from Table II into Eq. (7) are listed in Table III. According to the model considerations scale cracks should heal completely at and below these calculated strain-rate values. Table III also contains the values for the critical strain rates estimated from the results of the metallographic investigations. As seen from Table III, there is a surprisingly good agreement between values from the model calculations and the metallographic investigations. For the 18 Cr steel and the 24 Cr steel the (b)-values have to be compared to the values from the metallographic investigations, because both materials had shown oxide scale wrinkles. It could be argued that in partially detached scales crack healing need not necessarily occur at the detached tops for the restoration of the protective effect. Rather, the formation of new oxide on the metal surface

Table III. Critical strain rates for crack healing

	Model calculations	Metallographic investigations
18 Cr steel	(a) $1.2\times10^{-8}\,s^{-1}$	$<10^{-8}\,s^{-1}$
	(b) $5.2\times10^{-10}\,s^{-1}$	
24 Cr steel	(a) $3.7\times10^{-8}\,s^{-1}$	$10^{-7}\cdots10^{-8}\,s^{-1}$
	(b) $1.1\times10^{-8}\,s^{-1}$	
Alloy 800	(a) $5.3\times10^{-8}\,s^{-1}$	$10^{-7}\cdot\cdot10^{-8}\,s^{-1}$

beneath the detached and cracked part of the scale might again provide a protective scale, Fig. 6. However, it is assumed that the formation of new oxide will soon be slowed down below the detached scale since oxygen is consumed by oxidation, but the small crack opening does not allow a quick supply of oxygen from the surrounding atmosphere. The consequence will be an enrichment of corrosive elements beneath the detached scale and subsequent internal corrosion. Therefore, the critical strain rate should be determined mainly by the rate at which the scale crack is closed again by oxide growth at the crack faces. The results in Table III may be taken as a confirmation of this assumption.

SCALE CRACKING/HEALING MAPS

When knowing the values for the beginning of scale cracking (in the present case from Ref. 1) and the values of the critical strain rates for crack healing, "scale cracking/healing maps" can be constructed. These maps mark off the conditions for the following three cases:

I. No scale cracking.

II. Scale cracking but subsequent rapid healing preventing increased internal corrosion.

III. Scale cracking with the healing rate being too low compared to the applied strain rate for instant restoration of the protective effect.

The probability of damage by internal corrosion increases from I to III. Maps of this kind allow a classification of protective oxide scales concerning their protective effect during tensile straining. These maps may be helpful also in structural design for high-temperature applications since it can be estimated in which of the regions (I, II, or III) the anticipated deformation of the structure during service will be found.

"Scale cracking/healing maps" with the parameters strain ε_0 and strain rate $\dot{\varepsilon}_0$ have been constructed in Fig. 7 from the data of the steels discussed in this paper. The data include the experimental results as well as (for the critical strain rates) results from the model calculations (which were confirmed by the experimental results). The maps cover the investigated strain-rate region of 10^{-6} to $10^{-8}\,s^{-1}$. For the 18Cr-Ce steel the border between regions II and III could not be evaluated either by the experiments or by the model calculations. The experiments, however, showed that it should lie above $10^{-6}\,s^{-1}$. This border is shown in Fig. 7 together with a question mark indicating the uncertainty about its location.

As seen from these maps the scales with the lower strain values-to-cracking on Alloy 800 and on the 18Cr-Ce steel exhibit a great safety factor concerning corrosion protection as a consequence of their good healing qualities due to the absence of detached regions. The partially detached

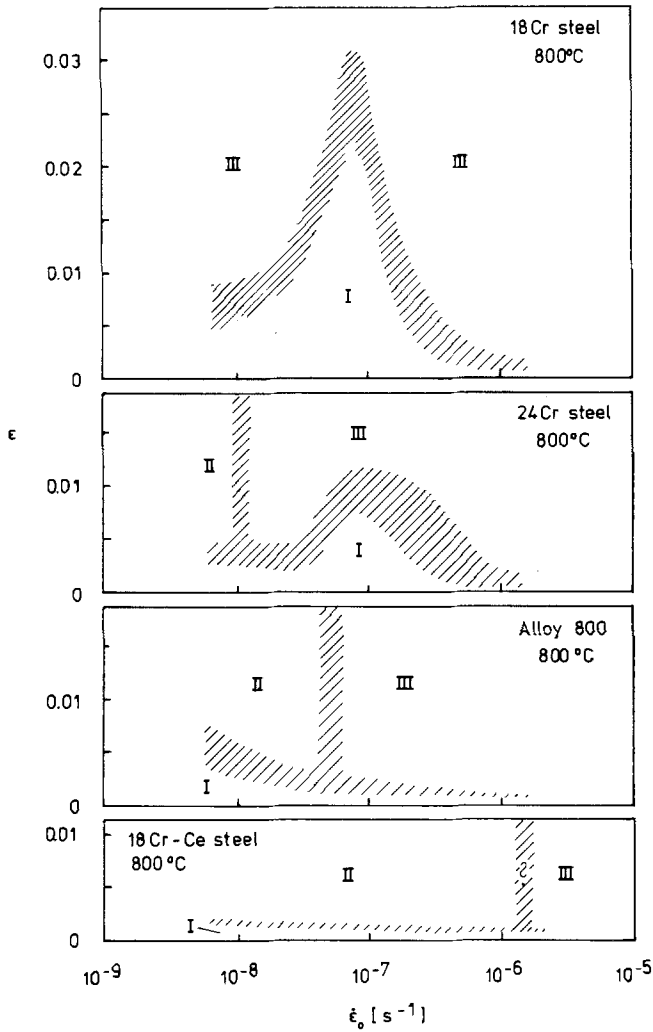

Fig. 7. Scale cracking/healing maps for the steels investigated. Details see text.

scale on the 24 Cr steel shows both a relatively high tensile strain to cracking but, nevertheless, acceptable healing qualities. The higher strains-to-cracking of the extensively detached scales on the 18 Cr steel, however, are associated with worse healing properties.

These results also allow a more general formulation. Oxide scales with marked, lateral, oxide-scale growth may exhibit larger strains to scale cracking under tensile deformation than those without lateral growth.[1] If

lateral growth, however, leads to extensive scale detachment, the healing capabilities of these scales are strongly degraded. Therefore, under the aspect of crack healing an adherent oxide scale is of great importance concerning the resistance against high-temperature corrosion in the presence of tensile stresses.

CONCLUSIONS

1. Optical evidence of oxide scale crack healing can be found in surface investigations as well as in investigations of the oxide scales in metallographic sections. Comparing the data for scale cracking and the course of internal corrosion also elucidates crack-healing processes.

2. The experimental results suggest the existence of a critical strain rate for crack healing. Below this strain rate, crack healing leads to an instant repair of the scale, thus preventing increased internal corrosion, although cracking of the scale has occurred. Above the critical strain rate increased corrosion is observed.

3. The existence of a critical strain rate for crack healing can be explained by model considerations. For the steels investigated in this paper results from the model calculations agree surprisingly well with the experimental data concerning this critical strain rate.

4. Adherent scales show better healing capabilities than (partially) detached scales.

5. On the basis of the scale cracking data and the healing data "scale cracking/healing maps" can be developed delineating the conditions for (a) no scale cracking; (b) scale cracking but instant scale repair by crack healing thus preserving the protective effect; (c) scale cracking with crack healing not being fast enough for preserving the protective effect.

Severe depletion of scale-forming elements in the base metal has not been considered in this paper. This aspect may play a role if scale cracking has occurred so many times that the content of these elements has decreased below a critical amount at which the protective effect of the newly formed parts of the scale no longer occurs. It is assumed that this situation can be represented by a critical strain value which should be a function of the applied strain rate. This value, however, had not been reached in the experiments discussed in this paper.

ACKNOWLEDGMENTS

Thanks are due to Prof. Rahmel for reading the manuscript and helpful discussions, those members of the technical staff of Dechema-Institut who

contributed to this work with their skillful assistance, and the Deutsche Forschungsgemeinschaft for financial support.

REFERENCES

1. M. Schütze, *Oxid. Met.* **24**, 199 (1985).
2. H. W. Grünling, B. Ilschner, S. Leistikow, A. Rahmel, and M. Schmidt, *Behaviour of High Temperature Alloys in Aggressive Environments* (The Metals Society, London, 1980), p. 869.
3. S. Leistikow and R. Kraft, *J. Mat. Tech.* **6**, 416 (1975).
4. Y. Ikeda and K. Nii, *J. Japan Instit. Met.* **47**, 191 (1983).
5. A. Schnaas and H. J. Grabke, *Oxid. Met.* **12**, 387 (1978).